Brain Topography (2026) 39:68
https://doi.org/10.1007/s10548-026-01220-8

ORIGINAL PAPER

Association Between Spatiotemporal Properties of Global Brain Activity and Childhood Emotional and Behavioral Problems: Evidence from Microstate C

Yan Hong[1,2] · Renlai Zhou[1,3,4]

Received: 19 March 2026 / Accepted: 30 May 2026

Abstract

This study aimed to examine the spatiotemporal properties of resting-state global brain network activity and their associations with emotional and behavioral functioning in children. Resting-state electroencephalography (EEG) was acquired in 83 children aged 6–7 years. Microstate features were extracted via K-means clustering, and partial least squares (PLS) regression was used to characterize multivariate associations between microstate temporal metrics (global explained variance, duration, occurrence, and coverage) and parent-rated scores on the Child Behavior Checklist (CBCL). Results demonstrated that four canonical microstate classes were already present in 6–7-year-old children, with microstate C showing dominance across temporal parameters. PLS revealed that the temporal parameters of microstate C were positively associated with total CBCL scores, whereas no significant relationships were observed for the other microstate classes. These findings suggest that neural dynamics indexed by microstate C may be associated with individual differences in emotional and behavioral regulation in 6–7-year-old children, highlighting its potential as an electrophysiological marker of neurobehavioral development.

Keywords EEG microstate · Resting-state network · Children · Emotional and behavioral functioning

Introduction

Childhood represents a critical window during which the brain undergoes rapid neuroanatomical and functional development. Neuroimaging evidence indicates that gray matter volume peaks at approximately 5.9 years of age, marking the culmination of synaptic pruning. In contrast, myelination of white matter fibers continues progressively to optimize the conduction efficiency and synchrony of neural networks (Bethlehem et al. 2022). During this period, children also undergo rapid advances in cognitive functioning (Sameroff and Haith 1996). The age of 6–7 years constitutes a pivotal transition from preschool to formal schooling, which imposes novel demands on executive functions, behavioral regulation, and socioemotional adjustment. Accordingly, this age range provides an ideal window for investigating the links between neural brain development and cognitive–behavioral functioning.

EEG microstate analysis represents a key approach for characterizing the spatiotemporal dynamics of large-scale brain networks (Michel and Koenig 2018). A central premise of this method is that the scalp potential field reflects momentary states of global neural activity, manifesting as brief episodes of synchronized neural activity that evolve dynamically over time. The "atoms of thought" hypothesis further proposes that microstates may correspond to distinct information-processing functions, such that individuals

Communicated by Urs Maurer.

✉ Renlai Zhou
rlzhou@nju.edu.cn

1 Department of Psychology, Nanjing University, Xianlin Avenue No. 163, Nanjing 210023, China

2 Zhejiang Philosophy and Social Science Laboratory for Research in Early Development and Childcare, Hangzhou Normal University, Hangzhou 311121, China

3 Department of Radiology, The Affiliated Drum Tower Hospital, Medical School of Nanjing University, Nanjing 210008, China

4 State Key Laboratory of Media Convergence Production Technology and Systems, Beijing 100803, China

exhibit different patterns of mental activity across microstates, and these enduring mental processes shape how external information is processed and responded to (Khanna et al. 2015; Lehmann et al. 1998). Resting-state EEG microstates are not only closely linked to higher cognitive functions and states of consciousness but also show robust associations with a wide range of psychiatric and neurological disorders in both children and adults (for reviews, see Khanna et al. 2015; Michel and Koenig 2018). Recent empirical studies and meta-analyses have linked altered microstate dynamics to conditions such as schizophrenia (da Cruz et al. 2020), attention-deficit/hyperactivity disorder (ADHD; Berchio et al. 2025), and affective disorders (Chivu et al., 2024; Luo et al. 2025; Vass et al. 2025).

Most studies of resting-state EEG have reported four identical canonical microstates that account for the majority of global topographic variability (Lehmann et al. 2009). Concurrent EEG-fMRI studies have demonstrated that the spatial patterns of these microstates resemble well-established resting-state networks (Bréchet et al. 2019). These four microstate classes, labeled A, B, C, and D, are hypothesized to represent the auditory, visual, default mode, and attention networks, respectively (Bréchet et al. 2019; Michel and Koenig 2018). Some studies have also reported additional microstate classes, such as microstate E (e.g., Michel and Koenig 2018). The high temporal resolution of electroencephalography enables quantification of temporal metrics for each resting-state network, conferring a unique advantage for characterizing global brain activity. Microstate analysis links fast-scale EEG dynamics to large-scale brain networks, offering a framework to study neural processes underlying cognition, emotion, and attention and to relate individual differences in brain dynamics to children's emotional, behavioral, and temperamental functioning.

EEG microstates undergo developmental changes beginning in infancy and gradually establish close links with behavior and higher-order cognitive functioning. Microstate topographies highly similar to those observed in adults emerge as early as 6–12 months of age, indicating that the foundational architecture of large-scale brain networks is already present and functional in early infancy (Ghosh et al. 2025; Gilbreath et al. 2025). Recent longitudinal evidence has identified conserved developmental trajectories of sensory-related microstates and a rapid acceleration of state transitions during the first two years of life (Ghosh et al. 2025), with these early functional dynamics appearing relatively resilient to variations in early dietary patterns (Gilbreath et al. 2025). As development progresses into early childhood, these patterns become more specialized. Bagdasarov et al. (2022) characterized the spatiotemporal properties of resting-state microstates in 4–8-year-old children and found that microstate C was temporally dominant, followed by microstate B, with sex and age differences observed for microstates C and D. Hill et al. (2023) further examined associations of temporal characteristics of resting-state microstates with age, biological sex, and alpha power in children aged 4–12 years. This study revealed that sex predicted temporal parameters of microstates A, C, D, and E. In addition, all four temporal metrics of microstate C were positively associated with alpha power. The sensitivity of these spatiotemporal parameters suggests that deviations in microstate patterns may reflect underlying neurodevelopmental variations, a premise that has led to a growing body of clinical research.

Reflecting their importance in neurodevelopment, clinical studies have demonstrated that EEG microstate features, together with source and connectivity measures, can help distinguish children with ADHD from neurotypical children (Berchio et al. 2025; Leon et al. 2025), and other work has proposed microstates as potential biomarkers for autism spectrum disorder (Ma et al. 2025). One clinical investigation identified microstate C as a neurophysiological biomarker for discriminating among states of consciousness in 5–6-year-old children (Zhang et al. 2025). While these studies highlight the potential of microstates as biomarkers for clinical conditions, their utility in characterizing the spectrum of functioning within neurotypical populations is also gaining attention. Emerging evidence has begun to link microstate parameters to cognitive and behavioral functional outcomes. Bagdasarov et al. (2024b) reported that in 4–8-year-old children, the error-related negativity (ERN) was positively correlated with global explained variance (GEV) of error-related microstate C, ERN was positively associated with GEV of resting-state microstate D, and GEV of error-related microstate C was positively correlated with GEV of resting-state microstate D, establishing a link between children's resting-state brain networks and error-processing responses during task performance. However, most studies linking microstates to children's behavior have focused either on clinical group comparisons or on specific cognitive tasks conducted under laboratory conditions. Consequently, it remains unclear how these neural dynamics relate to children's broader emotional and behavioral functioning in everyday life.

Existing studies on pediatric EEG microstates have largely focused on developmental profiles, describing the proportional occurrence of different microstate classes, examining developmental trends with age and sex, and establishing population-level developmental norms (Bagdasarov et al. 2022; Hill et al. 2023), including large-scale longitudinal efforts that have characterized conserved and context-specific maturation trends across culturally diverse cohorts (Ghosh et al. 2025). However, comparatively little research has examined how variability in these neural dynamics relates to individual differences in children's emotional and behavioral functioning. Bagdasarov et al. (2024b) linked microstates to specific cognitive abilities under laboratory conditions. Yet, it remains unclear whether these neural markers are associated with broader emotional and behavioral characteristics that manifest in children's everyday functioning. Recent work has begun to examine developmental trajectories of EEG microstates from infancy to middle childhood and their associations with behavioral outcomes (Kelsey et al. 2026). Nevertheless, how resting-state microstate dynamics relate to individual differences in children's emotional and behavioral functioning within specific developmental stages remains poorly understood. In recent years, researchers have begun investigating neurobiological correlates of broader emotional, behavioral, and temperamental characteristics in children (Xie et al. 2025), highlighting the importance of examining brain–behavior associations in community samples to better understand typical developmental variation.

Accordingly, the present study had two primary objectives. First, in a homogeneous sample of 6–7-year-old children, we aimed to characterize microstate topographies and their temporal properties to delineate global brain developmental status at this critical age. Second, using multidimensional parent-rated scales and partial least squares (PLS) regression as a multivariate statistical approach, we sought to identify coordinated covariance patterns between resting-state brain network dynamics and children's emotional, behavioral, and temperamental characteristics. Based on previous developmental microstate research, we hypothesized that 6–7-year-old children would exhibit a stable set of canonical microstate topographies, with microstate C already emerging as the dominant class during this developmental stage. Microstates C and D have been linked, respectively, to the default mode network (DMN) and the attention network, both of which are critical for emotional processing and behavioral regulation (Tarailis et al. 2024). Consequently, we predicted that the temporal parameters of these microstates would be significantly associated with individual differences in children's emotional and behavioral functioning, as well as temperamental traits such as effortful control. To capture a multifaceted profile of children's psychological functioning, we employed three complementary parent-report instruments. The Children's Behavior Questionnaire (CBQ; Putnam and Rothbart 2006) was used to assess relatively stable temperamental traits, providing an index of underlying dispositional tendencies. In contrast, the Child Behavior Checklist (CBCL; Achenbach 2001) and the Strengths and Difficulties Questionnaire (SDQ; Goodman 2001) primarily assess current emotional and behavioral symptoms. Importantly, the SDQ includes a prosocial behavior subscale that captures positive aspects of social functioning. Using these three measures together allowed us to distinguish temperament from current behavioral and emotional difficulties, while also considering both problem behaviors and positive social adjustment within the same multivariate framework.

Methods

Participants

First-grade children were recruited through voluntary parental registration. A total of 83 children completed data collection and questionnaire filling. Children's monthly age was calculated based on date of birth and testing; the final sample included in the analysis had a mean age of 81.70 ± 4.25 months. Among them, 49 were boys (59.04%), and 34 were girls (40.96%). This study was approved by the Psychology Study Ethics Committee of Nanjing University (Approval number: NJUPSY202209003). Informed written consent was provided by the caregivers of all participants. Parents also completed the corresponding questionnaires; after obtaining verbal consent from the children, EEG data collection was conducted.

All children were Han Chinese children residing in Liuhe District, Nanjing, Jiangsu Province. Specifically, 11 children had a rural household registration, and 72 had an urban household registration. Parental characteristics, including years of education (based on the age at which they completed schooling), income status (a continuous variable divided into 21 grades)[1], and subjective socioeconomic status (a ladder scale ranging from 1 to 10), are presented as follows: The average years of education were 14.48 ± 2.46 for fathers and 14.53 ± 2.31 for mothers. The average income score was 15.12 ± 3.11 for fathers. For mothers, 11 had no income, and the average income score of the remaining mothers was 11.17 ± 3.41. The average subjective socioeconomic status score was 6.23 ± 1.20.

Measurements

Children's emotional, behavioral, and temperamental characteristics were assessed using three parent-rated questionnaires.

[1] Average monthly income (Chinese Yuan, CNY) was measured on a 21-point scale with the following ranges: (1) 1–499; (2) 500–999; (3) 1,000–1,499; (4) 1,500–1,999; (5) 2,000–2499; (6) 2,500–2,999; (7) 3,000–3,499; (8) 3,500–3,999; (9) 4,000–4,499; (10) 4,500–4,999; (11) 5,000–5,999; (12) 6,000–6,999; (13) 7,000–7,999; (14) 8,000–8,999; (15) 9,000–9,999; (16) 10,000–12,000; (17) 12,000–15,000; (18) 15,000–20,000; (19) 20,000–25,000; (20) 25,000–30,000; (21) >30,000.

Child Behavioral Checklist (CBCL; Achenbach 2001). Parents completed the 113-item CBCL to report children's broad-spectrum behavioral and emotional problems as well as social competence, providing a detailed and clinically-standardized assessment of a wide spectrum of internalizing and externalizing behaviors. Items were rated on a 3-point Likert scale ranging from 0 = not true to 2 = very true or often true. The CBCL comprises nine subscales (withdrawn, somatic complaints, anxious/depressed, social problems, thought problems, attention problems, rule-breaking behavior, aggressive behavior, and sexual problems), from which internalizing (withdrawn, somatic Complaints, and Anxious/Depressed), externalizing (rule-Breaking and aggressive behavior), and total problem scores can be derived. The total problem scale has demonstrated good internal consistency (α = 0.80; Achenbach 2001). In the present study, the Cronbach's alpha coefficient was 0.90.

Children's Behavior Questionnaire (CBQ; Putnam and Rothbart 2006). Parents completed the 94-item short form of the CBQ to assess child temperament. This instrument focuses on individual differences in reactive and regulatory biological systems, providing a measure of dispositional traits that is distinct from the symptomatic focus of the CBCL and SDQ. Items were rated on a 7-point scale from 1 = extremely untrue to 7 = extremely true. The CBQ includes 15 subscales (activity level, anger/frustration, approach/positive anticipation, attentional focusing, discomfort, fear, emotional reactivity, high-intensity pleasure, impulsivity, inhibitory control, low-intensity pleasure, perceptual sensitivity, sadness, shyness, smiling/laughter, and soothability). Internal consistency for the subscales ranges from 0.61 to 0.85 (Putnam and Rothbart 2006). In the current study, the Cronbach's alpha coefficient for the full scale was 0.77.

Strengths and Difficulties Questionnaire (SDQ; Goodman 2001). Parents completed the 25-item SDQ, which serves as a brief behavioral screening tool and uniquely contributes a dimension of prosocial behavior not captured by the CBCL. Items were rated on a 3-point Likert scale from 0 = not true to 2 = certainly true. The SDQ consists of five factors: emotional symptoms, conduct problems, hyperactivity/inattention, peer relationship problems, and prosocial behavior. The scale has demonstrated acceptable internal consistency (α = 0.73; Goodman 2001). In the present study, the Cronbach's alpha coefficient was 0.84.

EEG Data Acquisition and Preprocessing

EEG data were collected from children in an empty classroom at their primary school. Previous studies have shown that approximately one-third of participants lose wakefulness and drift toward sleep within three minutes during resting-state scanning, highlighting the dynamic and unstable nature of the resting state (Tagliazucchi and Laufs 2014). To reduce fatigue and minimize the likelihood of drowsiness, the present study adopted an alternating eyes-open (EO) and eyes-closed (EC) resting-state paradigm (Ingram et al. 2024; Schiller et al. 2020). Referring to Hou et al. (2022), spontaneous EEG was recorded for a total of 8 min using eight alternating 1-minute blocks of EO and EC conditions. During EO blocks, children were instructed to fixate on a central cross presented on a computer screen while remaining relaxed and minimizing movements. Transitions between EO and EC blocks were guided by auditory instructions delivered via E-Prime. This block-wise alternating procedure was used to help children maintain attention and compliance throughout the recording session.

Due to occasional movement artifacts in a small number of children, the amount of artifact-free data within individual EO or EC blocks was sometimes limited. To maximize the amount of usable resting-state data while retaining all children in the analysis, EEG segments from EO and EC blocks were pooled before microstate analysis. The resulting dataset was therefore treated as a continuous resting-state recording reflecting the overall organization of spontaneous brain activity rather than condition-specific EO or EC dynamics.

EEG signals were recorded using a Neuroscan 32-channel Ag-AgCl electrode cap based on the international 10–20 system, with a Neuroscan NuAmps amplifier and online acquisition via Curry7 software. The sampling rate was set to 1024 Hz, and a band-pass filter of 0.05–100 Hz was applied online. All electrodes were referenced to AFz (the midpoint between FPz and Fz) during recording, and the input impedance of all recording electrodes was kept below 10 kΩ. Since the recording environment lacked electromagnetic shielding, a 50 Hz notch filter was applied during online acquisition, and an additional 50 Hz notch filter was implemented during offline processing to eliminate mains electrical interference.

Offline preprocessing was performed using MATLAB and the EEGLAB toolbox (Delorme and Makeig 2004; https://sccn.ucsd.edu/eeglab/index.php). The preprocessing pipeline included the following key steps. Continuous EEG signals were first band-pass filtered (0.1–40 Hz), and a notch filter (49–51 Hz) was applied to suppress power-line noise. The recording template included auxiliary electrooculography (EOG) channel positions; however, dedicated EOG electrodes were not attached during data acquisition to reduce preparation time and discomfort for the young children. These channels, therefore, contained no valid signal and were removed during preprocessing. Bilateral mastoid electrodes were also excluded before the microstate analysis. The remaining scalp EEG channels were re-referenced to the average reference and segmented into 2-s epochs. Noisy channels with persistent artifacts or poor contact were identified using an automated procedure supplemented by visual inspection. Identified bad channels were interpolated using spherical spline interpolation. On average, 1.05 ± 1.28 channels per participant were interpolated. Before independent component analysis (ICA), epochs containing obvious non-stationary artifacts, such as large low-frequency drifts or segments with abnormally large amplitudes, were identified through visual inspection and removed. ICA was then applied to identify and eliminate components associated with non-physiological artifacts (e.g., eye movements or muscle activity). On average, 2.86 ± 2.03 ICA components were removed per participant. Finally, remaining artifact-contaminated epochs were automatically rejected using a voltage threshold of ± 100 µV. After artifact rejection, an average of 16.54 ± 25.72 epochs per participant were discarded. Sufficient data remained for all children to ensure reliable microstate estimation.

Before microstate analysis, the preprocessed data were re-filtered with a 2 Hz high-pass and 20 Hz low-pass filter and down-sampled to 500 Hz. For each participant, the first 120 epochs (totaling 4 min of clean data) were selected following the original experimental sequence for subsequent analyses. This procedure ensured that all children contributed an identical data volume from a consistent temporal stage, following approaches used in previous developmental microstate studies (Bagdasarov et al. 2022). The selected duration also exceeds the minimum data length suggested for reliable microstate estimation (Liu et al. 2020).

Microstate Analysis

Microstate analysis was performed with Cartool (Brunet et al. 2011), following an individual-level to group-level analytical pipeline. For each child's EEG dataset, topographies were extracted specifically at the peaks of Global Field Power (GFP)—which reflects the variance of EEG potentials across all scalp electrodes and corresponds to time points at which the scalp topography is most stable (Brunet et al. 2011; Lehmann and Skrandies 1984). A modified k-means clustering analysis (polarity-invariant) was conducted on the pre-extracted GFP peaks of each participant, with 100 random initializations and the number of clusters ranging from 1 to 12. The optimal number of clusters for each individual was determined using the Meta-Criterion implemented in Cartool. This approach provides a consensus decision by integrating several independent indices, primarily focusing on Cross-Validation (CV), the Krzanowski–Lai (KL) index, and GEV, among others (Bagdasarov et al. 2024a, ; Bréchet et al. 2019).

At the group level, k-means clustering was applied to the optimal cluster sets identified for each child at the individual level. This group-level clustering was repeated 200 times, with the number of topographic clusters ranging from 1 to 15. The meta-criterion (Bréchet et al. 2019) was used to determine the optimal solution, which yielded 4 topographic clusters.

Finally, a back-fitting procedure was performed to fit the group-level microstate templates to individual raw data and extract temporal parameters. The correlation coefficient (ignoring polarity) between each time point and the group templates was calculated, and the microstate label corresponding to the highest correlation (≥ 50%) was assigned to that time point, a threshold consistent with established microstate back-fitting protocols (Michel and Koenig 2018). A sliding window (window width = 30 ms, Besag factor = 10) was used for temporal smoothing; microstate segments with a duration of less than 30 ms were merged and split into adjacent states (Murray et al. 2008; Pan et al. 2020). The back-fitting process generated four key temporal parameters for each microstate: GEV, duration, coverage, and occurrence rate.

Data Analysis

Scale data collation and correlational analyses were performed using Microsoft Excel 2019 and RStudio (R Core Team, 2023). The Shapiro-Wilk test was conducted to assess the normality of distribution, and homogeneity of variance was evaluated for four microstate metrics (GEV, duration, coverage, and occurrence rate). All four metrics exhibited non-normal distributions and heterogeneous variances; thus, Welch's one-way analysis of variance (ANOVA) was used to test for overall differences across microstate class (A–D). When ANOVA results indicated significant differences, pairwise comparisons were conducted using Welch's t-tests, with multiple comparisons corrected via the false discovery rate (FDR) method, and corrected *p*-values were reported. Cohen's d was calculated as the measure of effect size. Forest plots were generated using the ggplot2 package (version 3.5.1) in R.

Building upon the univariate characterization of microstate class distribution, we then employed a multivariate statistical approach to examine how these temporal dynamics relate to individual differences in psychological functioning. Specifically, PLS regression was used to identify robust covariance patterns between EEG microstate metrics and scale-measured emotional and behavioral functioning. Three independent PLS models were constructed to examine the associations between microstate metrics and scores from the CBCL, CBQ, and SDQ, respectively (Krishnan et al. 2011; Tomescu et al. 2022). PLS analyses were implemented in

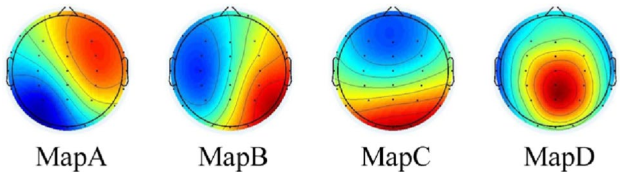

Fig. 1 Spatial characteristics of EEG microstates in children

Table 1 Descriptive statistics for temporal parameters of the four microstate classes

	MicrostateA	MicrostateB	MicrostateC	MicrostateD
GEV				
Mean (SD)	0.10 ± 0.03	0.08 ± 0.03	0.21 ± 0.05	0.09 ± 0.03
Range	0.03–0.25	0.02–0.16	0.04–0.33	0.03–0.21
Duration (ms)				
Mean (SD)	69.89 ± 4.87	69.10 ± 4.70	83.73 ± 7.20	69.61 ± 4.40
Range	59.14–93.79	59.41–81.20	61.34–100.98	61.67–82.75
Coverage (%)				
Mean (SD)	21.62 ± 5.07	21.67 ± 5.44	35.65 ± 6.51	21.06 ± 4.96
Range	9.83–43.79	8.75–35.69	11.47–49.46	10.76–33.79
Occurrence (per s)				
Mean (SD)	2.68 ± 0.40	2.71 ± 0.47	3.51 ± 0.33	2.62 ± 0.42
Range	1.54–3.78	1.35–3.68	1.72–4.05	1.57–3.58

RStudio using the mixOmics package (Rohart et al. 2017), with latent variables (LVs) extracted to model covariance between the predictor matrix X (microstate metrics) and the response matrix Y (emotional and behavioral functioning metrics); the number of LVs was set to 3, consistent with the PLS design of previous neuroimaging studies investigating brain-behavior associations (Krishnan et al. 2011). Composite factors explaining the covariance between X and Y matrices were derived by maximizing the decomposition of the covariance matrix between the predictor and response variables.

Permutation tests were then performed to assess the statistical significance of each LV: 1000 random permutations of the Y matrix samples were conducted, and PLS was re-run for each permutation to calculate the covariance between LVs of X and Y. The original covariance was compared against the distribution of permuted covariances to compute uncorrected p-values. The Benjamini-Hochberg method was applied to correct p-values for all LVs for FDR, with a significance threshold set at $q < 0.05$; only statistically significant LVs were retained for subsequent analyses.

The reliability of variable-LV correlations was evaluated via bootstrapping: 500 bootstrap resamples (with replacement) were performed, and the PLS model and correlation coefficients were recalculated for each resample. Standardized Z-scores were computed based on the bootstrap distribution: the original correlation coefficient was divided by its bootstrap standard deviation to obtain the Z-score, and two-tailed p-values were derived from the standard normal distribution. Finally, stratified FDR correction was applied to the p-values of variables within each significant LV.

Results

The meta-criterion for determining the optimal number of microstates revealed four canonical microstate maps labeled Maps A–D (Fig. 1). Descriptive statistics for the temporal parameters of each microstate are presented in Table 1.

Significant differences among microstate classes (A–D) were observed for all temporal parameters.

For GEV, Welch's ANOVA revealed a significant main effect of microstate class, $F(3, 179.73) = 134.76$, $p < 0.001$, $\omega^2 = 0.686$. Post-hoc comparisons indicated that Class C showed significantly higher GEV than Classes A, B, and D (all $ps < 0.001$). In addition, Classes A and D exhibited higher GEV than Class B ($ps < 0.001$), whereas no significant difference was observed between Classes A and D ($p = 0.324$).

A similar pattern was observed for the remaining temporal parameters: duration, coverage, and occurrence. Significant main effects were found for duration, $F(3, 180.32) = 94.29$, $p < 0.001$, $\omega^2 = 0.603$; coverage, $F(3, 181.46) = 108.66$, $p < 0.001$, $\omega^2 = 0.635$; and occurrence, $F(3, 180.89) = 115.82$, $p < 0.001$, $\omega^2 = 0.651$. In all cases, Microstate C exhibited significantly greater values than the other classes, while the remaining microstate classes did not differ significantly from each other.

Full pairwise comparison statistics are provided in the Supplementary Materials.

Figure 2A shows boxplots and pairwise comparisons for GEV. Figure 2B shows boxplots and pairwise comparisons for duration. Figure 2C shows boxplots and pairwise comparisons for coverage. Figure 2D shows boxplots and pairwise comparisons for occurrence rate.

Correlation Analysis

Shapiro-Wilk normality tests were conducted for CBCL subscales and total scores, and all variables violated normality assumptions (detailed results and normality test statistics are presented in the Supplementary Materials). Based on the data distribution, three subscales (somatic complaints, thought problems, and sexual problems) were excluded because their median and interquartile ranges were zero, indicating almost no variability in these variables. Variables with near-zero variance provide little information for multivariate modeling and may bias parameter estimation;

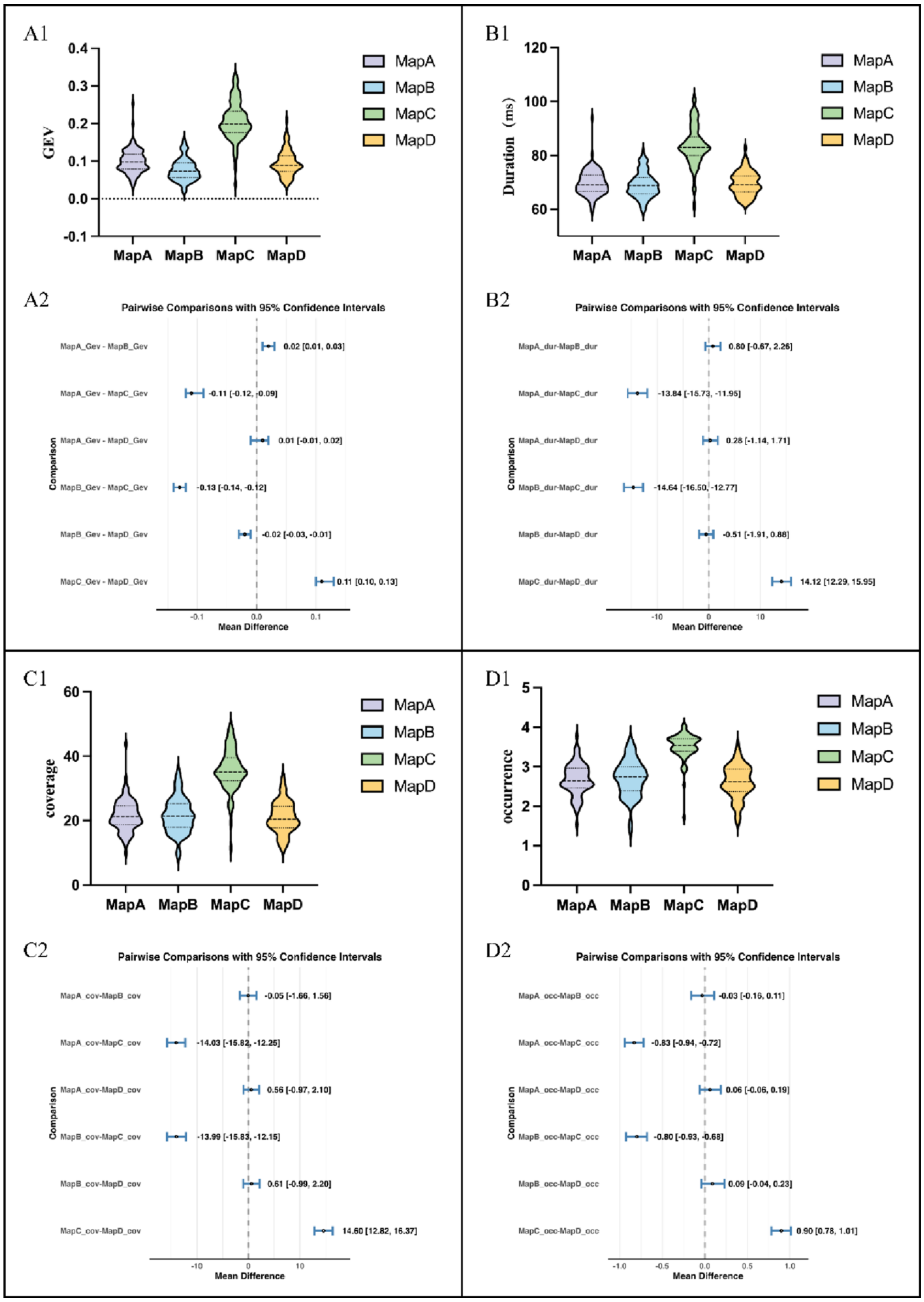

Fig. 2 Boxplots and pairwise comparisons of temporal characteristics of EEG microstates in children

therefore, these subscales were removed from subsequent analyses. Consequently, the operationalization of "behavioral and emotional symptoms" in the present study primarily reflects the most prevalent and variable symptom domains within a typical developmental cohort. Winsorization was applied to extreme values for all remaining subscales at the 2.5% and 97.5% levels (total 5% trimmed). Skewness was then examined, and variables with absolute skewness greater than 1 were transformed using the Yeo-Johnson transformation (Yeo and Johnson 2000). All variables were Z-standardized before PLS regression.

PLS analysis identified one significant latent variable (LV1), revealing an alignment between neural dynamics and behavioral profiles (canonical $r=0.402$; corrected $p=0.009$; Fig. 3). This LV1 explained 34.73% and 60.45% of the variance in the X matrix (microstate metrics) and Y matrix (CBCL scores), respectively, while accounting for 66.66% of the total covariance. The significant microstate metrics for Map C included all four temporal parameters

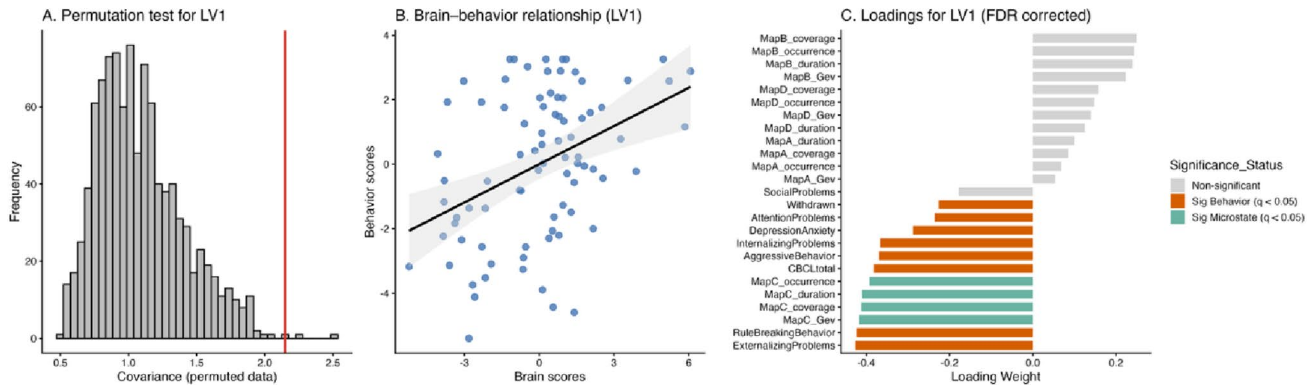

Fig. 3 Brain–behavior associations identified by PLS analysis

Table 2 PLS regression analysis of microstate metrics and CBCL scores, and results of significant correlations with Latent Variable 1 (LV1)

	95% Confidence Interval	FDR-corrected q Value	Loadings	VIP Values
X matrix variables				
MapC_Gev	[-0.459, -0.276]	<0.001	-0.412	1.648
MapC_duration	[-0.454, -0.264]	<0.001	-0.410	1.641
MapC_coverage	[-0.434, -0.267]	<0.001	-0.417	1.668
MapC_occurrence	[-0.468, -0.203]	<0.001	-0.392	1.570
Y Matrix variables				
Withdrawn	[-0.408, -0.053]	0.018	-0.226	/
Depression/Anxiety	[-0.440, -0.079]	0.003	-0.288	/
Social problems	[-0.338, 0.036]	0.085	-0.178	/
Attention problems	[-0.432, 0.010]	0.048	-0.236	/
Rule breaking behavior	[-0.559, -0.198]	<0.001	-0.423	/
Aggressive behavior	[-0.465, -0.223]	<0.001	-0.370	/
Internalizing problems	[-0.486, -0.223]	<0.001	-0.366	/
Externalizing problems	[-0.512, -0.288]	<0.001	-0.427	/
CBCL total	[-0.435, -0.304]	<0.001	-0.382	/

CBCL = Child Behavior Checklist. Internalizing Symptoms represent overcontrolled emotional distress, encompassing the Withdrawn and Somatic Complaints subscales, plus specific anxiety and depression items. Externalizing Symptoms represent under controlled or maladaptive behaviors, encompassing Rule-Breaking and Aggressive Behavior subscales. Higher scores across these indices reflect greater symptom severity and potential challenges in behavioral and emotional adjustment.

(GEV, duration, coverage, and occurrence rate) and were strongly associated with LV1, alongside the included CBCL scores.

All variables showed significant negative loadings on LV1, indicating a positive association between Map C metrics and CBCL scores: higher Map C parameter values were associated with higher levels of emotional and behavioral symptoms. All results survived multiple testing correction, supporting the robustness of the findings. LV1 significantly explained the covariance between X and Y variables, and the overall model was statistically significant. Detailed variable-specific correlations, confidence intervals, VIP values for X variables, and loadings for Y variables are presented in Table 2.

Figure 3A shows the permutation test results assessing the statistical significance of the first latent variable (LV1), where the histogram represents the null distribution of covariance from 1000 permutations and the red line indicates the observed covariance. Figure 3B illustrates the positive association between brain scores and behavioral scores for LV1, with each point representing an individual's latent variate score. The scores were computed by projecting the original brain and behavioral data onto their respective weight vectors derived from the PLS model, which were optimized to maximize the covariance between the two data blocks. The solid line and shaded area represent the least-squares regression fit and its 95% confidence interval, respectively. Figure 3C shows the variables' contribution to LV1. The bar plot illustrates the loading weights of microstate parameters and CBCL subscales on the LV1. Colored bars indicate variables that significantly contributed to the model after FDR correction ($q < 0.05$), while grey bars represent non-significant variables. The direction of the bars reflects the orientation of the association within the brain-behavior axis.

PLS regression was conducted between CBQ measures and microstate metrics. Following FDR correction, no significant LVs were identified at the threshold of $q < 0.05$.

Similarly, PLS regression was performed between SDQ scores and microstate metrics. After FDR correction, no significant LVs emerged at the $q < 0.05$ level.

Detailed summary statistics, including variance explained and VIP values for all tested LVs, are provided in the Supplementary Materials.

Discussion

The present study aimed to validate microstate patterns and their temporal characteristics in a sample of 6–7-year-old children, and to explore the associations between microstate temporal metrics and children's behavioral and temperamental traits. Consistent with our hypotheses, the results revealed that 6–7-year-old children exhibited the four canonical microstate classes that constitute the fundamental architecture of resting-state brain dynamics. Among these, microstate C was the temporally dominant class, consistent with observations in other pediatric cohorts, while no significant differences were found among the other three microstate classes. PLS regression analysis identified a significant positive association between temporal parameters of microstate C and children's symptom profiles, indicating that higher levels of microstate C were associated with greater symptom severity. Additionally, no significant associations were observed between other microstate classes and scores from the other behavioral or temperamental scales measured in this study.

The present study found that the four-microstate model was the optimal solution in 6–7-year-old children. This result is consistent with most adult studies (Michel and Koenig 2018) and the findings of Bagdasarov et al. (2022). However, the number of identified microstate classes can vary considerably across studies due to differences in sample characteristics, preprocessing procedures, clustering strategies, and model selection criteria. Recent large-scale studies in both adults and children have frequently reported five- or six-class solutions (Bagdasarov et al. , 2024b; Hill et al. 2023; Koenig et al. 2024; Zanesco 2024). Nevertheless, in terms of temporal dynamics, microstate C showed clear predominance across all temporal parameters in the present sample, consistent with prior large-scale findings (Zanesco 2024), whereas the remaining microstates (A, B, and D) showed relatively similar temporal characteristics without marked differentiation. This pattern may suggest that large-scale networks associated with microstate C, particularly the DMN, play a relatively prominent role in resting-state brain dynamics during this developmental stage. This is slightly different from Bagdasarov et al. (2022), who found that the parameters of microstate B were slightly higher than those of microstates A and D. This subtle difference is most likely due to variations in the methods used to acquire and analyze resting-state data. The present study adopted an alternating eyes-open and eyes-closed recording paradigm to obtain more comprehensive resting-state data with higher ecological validity. In contrast, the study by Bagdasarov et al. (2022) only analyzed the eyes-closed condition. Existing evidence has shown that the presence or absence of visual input can significantly alter brain oscillation rhythms and functional connectivity patterns, thereby directly affecting the topographic characteristics and temporal parameters of microstates (Khanna et al. 2015).

The present study found that temporal parameters of microstate C were significantly dominant in 6–7-year-old children, and higher levels of microstate C activity were associated with increased emotional and behavioral symptoms, particularly externalizing symptoms measured by the CBCL. In this context, externalizing symptoms primarily reflect overt behavioral difficulties such as rule-breaking and aggression, whereas internalizing symptoms capture more inwardly directed problems such as anxiety, depression, and social withdrawal. Within current functional interpretations, microstate C has been increasingly linked to large-scale brain networks supporting internally oriented processing, most commonly the DMN (Bagdasarov et al. 2022; Michel and Koenig 2018; Tarailis et al. 2024; Norouzi and Daliri 2025). Earlier EEG–fMRI work also associated this microstate with the salience network, although subsequent methodological reviews suggest that such mappings are sensitive to analytic strategies and sample characteristics (Tarailis et al. 2024). Thus, although microstate C is often discussed in relation to DMN dynamics, its functional significance is unlikely to reflect a strict one-to-one correspondence with a single resting-state network and may instead reflect coordinated interactions among multiple large-scale brain systems (Zanesco 2024). Within this broader framework, microstate C has been related to self-referential cognition, social cognition, and emotional regulation (Michel and Koenig 2018; Tarailis et al. 2024; Norouzi and Daliri 2025). Against this background, our findings suggest that individual differences in the temporal dynamics of microstate C are meaningfully related to variability in children's emotional and behavioral functioning. A tentative interpretation is that the temporal predominance of microstate C in some children may reflect a bias toward internally oriented processing at rest, accompanied by reduced flexibility in reallocating neural resources between internal and external modes. In turn, such a bias could be associated with less efficient monitoring of external cues and higher levels of emotional and behavioral problems, particularly externalizing difficulties involving impulsive or poorly regulated responses. This perspective is consistent with task-based studies in which greater pre-task coverage of microstate C has been linked to less efficient behavioral performance (Penalver-Andres et al. 2024), and with recent longitudinal evidence indicating that microstate temporal parameters are prospectively associated with behavioral outcomes across early childhood (Kelsey et al. 2026). These interpretations should nonetheless be considered cautiously. The mapping between EEG microstates and functional networks is not strictly one-to-one, and the present data are correlational, precluding strong conclusions about mechanism or directionality.

Microstate D is considered to be closely associated with the dorsal attention network (Michel and Koenig 2018) and the frontoparietal network (Bréchet et al. 2019), and is mainly linked to executive functions such as working memory, cognitive control, and attentional control (Tarailis et al. 2024). The present study did not find an association between children's behavior, temperament, and microstate D, a result that reflects that the function of microstate D may be more reflected in the efficiency of performing specific cognitive tasks. For example, Bagdasarov et al. (2024b) found that the GEV of resting-state microstate D was positively correlated with ERN, but its association with broader emotional and behavioral symptom profiles and temperamental traits was not close enough. In addition, the frontoparietal control network, mainly involved in microstate D, is still in a rapid development stage in 6–7-year-old children (Casey et al. 2000) and has not yet formed a stable pattern, which may be asynchronous with the development of emotion and behavior. This result also suggests that the DMN associated with microstate C might play a more fundamental role in emotion and social cognition; its development may be relatively earlier, and its association with behavioral and emotional symptoms is potentially more direct and stable. The present study did not observe significant associations between children's behavioral or temperamental measures and microstates A or B. One possible explanation is that these microstates are often linked to basic sensory processing systems, particularly visual and auditory networks (e.g., Britz et al. 2010; Michel and Koenig 2018), which may be less directly related to the emotional and behavioral characteristics examined here. More broadly, the lack of significant associations for microstates A, B, and D should be interpreted with caution. These null findings may not only reflect distinct functional specializations but could also be influenced by factors such as limited statistical power, measurement sensitivity, or developmental stage–specific expressions of these neural signatures.

The present study has several limitations that should be acknowledged. First, this study adopted a cross-sectional design. Although it revealed the association between resting-state EEG microstates and children's emotional and behavioral symptoms, it cannot infer the direction of causality. Future studies could adopt a longitudinal follow-up design to further clarify whether the maturity of neural development leads to improved behavior or whether good behavioral performance promotes the development of brain function. Second, the sample size of this study is limited, and all children were from the same primary school in China, with a relatively homogeneous socioeconomic background. Although this design helps control confounding factors related to the social environment and enhances the internal consistency of the results, it inevitably limits the generalizability of the conclusions to broader child populations. Notably, recent large-scale longitudinal research in Western cohorts has revealed complex developmental trajectories of EEG microstates and their associations with behavior, but these samples have been predominantly non-Hispanic White and from middle-to-high socioeconomic backgrounds (Kelsey et al. 2026). In light of evidence that microstate dynamics and related neurodevelopmental patterns may be shaped by cultural and environmental contexts, future studies should verify and extend the present findings in larger samples drawn from more diverse cultural and socioeconomic backgrounds. Such cross-cultural comparisons will be essential for determining which aspects of microstate–behavior associations are universal and which are context-specific. In addition to sample characteristics, the behavioral assessment in the present study also reflects the symptom distribution typical of a community-based cohort. Because several CBCL subscales exhibited extremely limited variability in this sample, the analyses primarily focused on subscales with sufficient statistical variance. As a result, the present findings mainly characterize the brain–behavior relationships associated with more common emotional and behavioral challenges in early childhood. Future studies including clinical samples with higher symptom severity will be important for determining whether resting-state microstate dynamics are also associated with less frequent but clinically more severe domains, such as thought or somatic problems. Finally, from a methodological perspective, the present study utilized an alternating EO/EC paradigm but did not examine their distinct contributions to microstate dynamics. Instead, the EO and EC segments were combined to characterize an overall resting-state profile. Given the potential differences between EO and EC states, future developmental research should aim to collect longer recordings to directly contrast these two conditions. In addition, although EEG technology has high temporal resolution, its spatial resolution is relatively limited. It is expected that future studies can combine high-density EEG, multimodal neuroimaging technologies (e.g., fMRI), or source localization methods to more in-depth and comprehensively reveal the associations between microstates and children's cognitive, emotional, and behavioral development on the basis of clarifying the intracerebral generators of microstates.

In summary, the present study employed resting-state EEG microstate analysis to characterize the spatiotemporal dynamic characteristics of global brain activity in 6–7-year-old children, and further explored its associations with emotional and behavioral characteristics. The findings reveal that 6–7-year-old children already exhibit the four canonical microstate patterns, with microstate C emerging as the dominant class at the group level. This pattern suggests that key aspects of large-scale brain network organization may already be taking shape by this developmental stage. PLS analysis further revealed that the temporal parameters of microstate C were associated with higher levels of emotional and behavioral symptoms, particularly externalizing symptoms measured by the CBCL, indicating that microstate C dynamics are linked to individual differences in behavioral and emotional functioning in 6–7-year-old children. From a large-scale network perspective, these associations may reflect variations in the functional dynamics of networks often linked to microstate C, such as the DMN and related systems. Although the present findings are correlational and should be interpreted cautiously, they provide preliminary evidence that resting-state microstate dynamics may serve as useful neural indicators of children's emotional and behavioral functioning. Future longitudinal and multimodal studies will be necessary to clarify the developmental significance and potential functional mechanisms underlying these associations.

Supplementary Information The online version contains supplementary material available at https://doi.org/10.1007/s10548-026-01220-8.

Author Contributions Yan hong: Conceptualization, Methodology, Software, Formal analysis, Investigation, Writing - Original Draft, Writing – review & editing, Visualization. Renlai Zhou: Conceptualization, Methodology, Validation, Resources, Writing - Review & Editing, Supervision, Project administration, Funding acquisition.

Funding sources This study was supported by SpaceMedical Experiment Project of CMSP (HYZHXMR01006).

Data Availability The datasets generated for this research are available on request to the corresponding author.

Declarations

Competing interests The authors declare no competing interests.

References

Achenbach TM (2001) Achenbach system of empirically based assessment: School age forms and profiles, child behavior checklist for ages 6–18. Aseba

Bagdasarov A, Roberts K, Bréchet L, Brunet D, Michel CM, Gaffrey MS (2022) Spatiotemporal dynamics of EEG microstates in four- to eight-year-old children: Age- and sex-related effects. Dev Cogn Neurosci 57:101134. https://doi.org/10.1016/j.dcn.2022.101134

Bagdasarov A, Brunet D, Michel CM, Gaffrey MS (2024a) Microstate Analysis of Continuous Infant EEG: Tutorial and Reliability. Brain Topogr 37(4):496–513. https://doi.org/10.1007/s10548-024-01043-5

Bagdasarov A, Roberts K, Brunet D, Michel CM, Gaffrey MS (2024b) Exploring the Association Between EEG Microstates During Resting-State and Error-Related Activity in Young Children. Brain Topogr 37(4):552–570. https://doi.org/10.1007/s10548-023-01030-2

Berchio C, Kumar SS, Narzisi A, Fabbri-Destro M (2025) EEG Microstates in the Study of Attention-Deficit Hyperactivity Disorder: A Review of Preliminary Evidence. Psychophysiology 62(1):e14762. https://doi.org/10.1111/psyp.14762

Bethlehem RAI, Seidlitz J, White SR, Vogel JW, Anderson KM, Adamson C, Adler S, Alexopoulos GS, Anagnostou E, Areces-Gonzalez A, Astle DE, Auyeung B, Ayub M, Bae J, Ball G, Baron-Cohen S, Beare R, Bedford SA, Benegal V … Vetsa (2022). Brain charts for the human lifespan. *Nature*, *604*(7906), 525–533. https://doi.org/10.1038/s41586-022-04554-y

Bréchet L, Brunet D, Birot G, Gruetter R, Michel CM, Jorge J (2019) Capturing the spatiotemporal dynamics of self-generated, task-initiated thoughts with EEG and fMRI. NeuroImage 194:82–92. https://doi.org/10.1016/j.neuroimage.2019.03.029

Britz J, Van De Ville D, Michel CM (2010) BOLD correlates of EEG topography reveal rapid resting-state network dynamics. NeuroImage 52(4):1162–1170. https://doi.org/10.1016/j.neuroimage.2010.02.052

Brunet D, Murray MM, Michel CM (2011) Spatiotemporal Analysis of Multichannel EEG: CARTOOL. Comput Intell Neurosci 2011(1):813870. https://doi.org/10.1155/2011/813870

Casey BJ, Giedd JN, Thomas KM (2000) Structural and functional brain development and its relation to cognitive development. Biol Psychol 54(1):241–257. https://doi.org/10.1016/S0301-0511(00)00058-2

Chivu, A., Pascal, S. A.,Damborskáá, A., & Tomescu, M. I. (2024). EEG Microstates in Mood and Anxiety Disorders: A Meta-analysis. Brain Topography, 37(3), 357-368. https://doi.org/10.1007/s10548-023-00999-0

da Cruz JR, Favrod O, Roinishvili M, Chkonia E, Brand A, Mohr C, Figueiredo P, Herzog MH (2020) EEG microstates are a candidate endophenotype for schizophrenia. Nat Commun 11(1):3089. https://doi.org/10.1038/s41467-020-16914-1

Delorme A, Makeig S (2004) EEGLAB: an open source toolbox for analysis of singletrial EEG dynamics including independent component analysis. J Neurosci Methods 134(1):9–21. https://doi.org/10.1016/j.jneumeth.2003.10.009

Ghosh P, Donald KA, Polanczyk GV, Rodriguez JP, Shephard E, Gabard-Durnam LJ, The Leap kD EEG Working Group (2025) Spatiotemporal dynamics of EEG microstate networks over the first two years of life: A multi-cohort longitudinal study. Imaging Neurosci 3:IMAGa59. https://doi.org/10.1162/IMAG.a.59

Gilbreath D, Hagood D, Andres A, Larson-Prior LJ (2025) The effect of diet on the development of EEG microstates in healthy infant throughout the first year of life. NeuroImage 311:121152. https://doi.org/10.1016/j.neuroimage.2025.121152

Goodman R (2001) Psychometric Properties of the Strengths and Difficulties Questionnaire. J Am Acad Child Adolesc Psychiatry 40(11):1337–1345. https://doi.org/10.1097/00004583-200111000-00015

Hill AT, Bailey NW, Zomorrodi R, Hadas I, Kirkovski M, Das S, Lum JAG, Enticott PG (2023) EEG microstates in early-to-middle childhood show associations with age, biological sex, and alpha power. Hum Brain Mapp 44(18):6484–6498. https://doi.org/10.1002/hbm.26525

Hou L, Chen L, Zhou R (2022) Premenstrual syndrome is associated with an altered spontaneous electroencephalographic delta/beta power ratio across the menstrual cycle. Int J Psychophysiol 181:64–72. https://doi.org/10.1016/j.ijpsycho.2022.08.007

Ingram BT, Mayhew SD, Bagshaw AP (2024) Brain state dynamics differ between eyes open and eyes closed rest. Hum Brain Mapp 45(10):e26746. https://doi.org/10.1002/hbm.26746

Kelsey C, Sacks DD, Abron A, Vartany P, Mulligan K, Bosquet Enlow M, Nelson CA (2026) The development of electroencephalography microstates from infancy into middle childhood and their associations with behavior. *Developmental Psychology*, Advance online publicationhttps://doi.org/10.1037/dev0002183

Khanna A, Pascual-Leone A, Michel CM, Farzan F (2015) Microstates in resting-state EEG: Current status and future directions. Neurosci Biobehavioral Reviews 49:105–113. https://doi.org/10.1016/j.neubiorev.2014.12.010

Koenig T, Diezig S, Kalburgi SN, Antonova E, Artoni F, Brechet L, Britz J, Croce P, Custo A, Damborská A, Deolindo C, Heinrichs M, Kleinert T, Liang Z, Murphy MM, Nash K, Nehaniv C, Schiller B, Smailovic U, Michel CM (2024) EEG-Meta-Microstates: Towards a More Objective Use of Resting-State EEG Microstate Findings Across Studies. Brain Topogr 37(2):218–231. https://doi.org/10.1007/s10548-023-00993-6

Krishnan A, Williams LJ, McIntosh AR, Abdi H (2011) Partial Least Squares (PLS) methods for neuroimaging: A tutorial and review. NeuroImage 56(2):455–475. https://doi.org/10.1016/j.neuroimage.2010.07.034

Lehmann D, Skrandies W (1984) Spatial analysis of evoked potentials in man–a review. Prog Neurobiol 23(3):227–250. https://doi.org/10.1016/0301-0082(84)90003-0

Lehmann D, Strik WK, Henggeler B, Koenig T, Koukkou M (1998) Brain electric microstates and momentary conscious mind states as building blocks of spontaneous thinking: I. Visual imagery and abstract thoughts. Int J Psychophysiol 29(1):1–11. https://doi.org/10.1016/S0167-8760(97)00098-6

Lehmann D, Pascual-Marqui RD, Michel C (2009) EEG microstates. Scholarpedia 4(3):7632

Leon C, Kaur S, Sagar R, Tayade P, Sharma R (2025) Cortical Hypoactivation of Frontal Areas Modulates Resting Electroencephalography Microstates in Children With Attention-Deficit/Hyperactivity Disorder. Biol Psychiatry: Cogn Neurosci Neuroimaging 10(6):565–573. https://doi.org/10.1016/j.bpsc.2024.11.012

Liu J, Xu J, Zou G, He Y, Zou Q, Gao J-H (2020) Reliability and Individual Specificity of EEG Microstate Characteristics. Brain Topogr 33(4):438–449. https://doi.org/10.1007/s10548-020-00777-2

Luo Y, Shen Y, Fan X (2025) EEG microstates in adolescent depression: Effects of depression severity and overall symptoms. J Affect Disord 390:119819. https://doi.org/10.1016/j.jad.2025.119819

Ma M, Yang Z, Wang L, Lu S, Han J, Li X (2025) Resting Electroencephalography Microstates and Alpha Power Modulation in Preschool-Aged Children with Autism Spectrum Disorder. Brain Sci 15(6):544. https://doi.org/10.3390/brainsci15060544

Michel CM, Koenig T (2018) EEG microstates as a tool for studying the temporal dynamics of whole-brain neuronal networks: A review. NeuroImage 180:577–593. https://doi.org/10.1016/j.neuroimage.2017.11.062

Murray MM, Brunet D, Michel CM (2008) Topographic ERP Analyses: A Step-by-Step Tutorial Review. Brain Topogr 20(4):249–264. https://doi.org/10.1007/s10548-008-0054-5

Norouzi H, Daliri MR (2025) Microstate Dynamics in Working Memory: Exploring Spatial Information Coding of Stimulus and Behavioral Performance. Brain Behav 15(8):e70765. https://doi.org/10.1002/brb3.70765

Pan D-n, Hoid D, Gu R-l, Li X (2020) Emotional working memory training reduces rumination and alters the EEG microstate in anxious individuals. NeuroImage: Clin 28:102488. https://doi.org/10.1016/j.nicl.2020.102488

Penalver-Andres JA, Buetler KA, Koenig T, Müri RM, Marchal-Crespo L (2024) Resting-State Functional Networks Correlate with Motor Performance in a Complex Visuomotor Task: An EEG Microstate Pilot Study on Healthy Individuals. Brain Topogr 37(4):590–607. https://doi.org/10.1007/s10548-022-00934-9

Putnam SP, Rothbart MK (2006) Development of Short and Very Short Forms of the Children's Behavior Questionnaire. J Pers Assess 87(1):102–112. https://doi.org/10.1207/s15327752jpa8701_09

Rohart F, Gautier B, Singh A, Lê Cao K-A (2017) mixOmics: An R package for 'omics feature selection and multiple data integration. PLoS Comput Biol 13(11):e1005752. https://doi.org/10.1371/journal.pcbi.1005752

Sameroff AJ, Haith MM (1996) The five to seven year shift. University of Chicago Press

Schiller B, Kleinert T, Teige-Mocigemba S, Klauer KC, Heinrichs M (2020) Temporal dynamics of resting EEG networks are associated with prosociality. Sci Rep 10(1):13066. https://doi.org/10.1038/s41598-020-69999-5

Tagliazucchi, E., & Laufs, H. (2014). Decoding Wakefulness Levels from Typical fMRI Resting-State Data Reveals Reliable Drifts between Wakefulness and Sleep. *Neuron*, *82*(3), 695–708. https://doi.org/10.1016/j.neuron.2014.03.020.

Tarailis P, Koenig T, Michel CM, Griškova-Bulanova I (2024) The Functional Aspects of Resting EEG Microstates: A Systematic Review. Brain Topogr 37(2):181–217. https://doi.org/10.1007/s10548-023-00958-9

Tomescu MI, Papasteri CC, Sofonea A, Boldasu R, Kebets V, Pistol CAD, Poalelungi C, Benescu V, Podina IR, Nedelcea CI, Berceanu AI, Carcea I (2022) Spontaneous thought and microstate activity modulation by social imitation. NeuroImage 249:118878. https://doi.org/10.1016/j.neuroimage.2022.118878

R Core Team. (2023). R: A language and environment for statistical computing. R Foundation for StatisticalComputing. https://www.R-project.org/

Vass Á, Farkas K, Lányi O, Kói T, Csukly G, Réthelyi JM, Baradits M (2025) Current Status of Electroencephalography Microstate in Psychiatric Disorders: A Systematic Review and Meta-Analysis. Biol Psychiatry: Cogn Neurosci Neuroimaging 10(10):1015–1024. https://doi.org/10.1016/j.bpsc.2025.04.001

Xie W, Wang Y, Sacks DD, Nelson CA, Enlow B, M (2025) Neural correlates of child temperament: The role of brain network connectivity in psychopathology risk. J Child Psychol Psychiatry. https://doi.org/10.1111/jcpp.70095

Yeo IK, Johnson RA (2000) A new family of power transformations to improve normality or symmetry. Biometrika 87(4):954–959. https://doi.org/10.1093/biomet/87.4.954

Zanesco AP (2024) Normative Temporal Dynamics of Resting EEG Microstates. Brain Topogr 37(2):243–264. https://doi.org/10.1007/s10548-023-01004-4

Zhang Y, Hui Z, Su Y, Qi W, Zhang G, Zhou L, Zhang J, Shi K, Yang Y, Yang L, Chen G, Li S, Wang M, Zhu D (2025) EEG microstate analysis in children with prolonged disorders of consciousness. Sci Rep 15(1):26148. https://doi.org/10.1038/s41598-025-11038-2